COB-2019-0453
HIDRODYNAMICS OF FISH SWIMMING IN *QUASI*-STEADY FLOW REGIME

Antônio Augusto Nogueira Espenchitt
Marianela Machuca Macias
Taygoara Felamingo de Oliveira
Antonio Cesar Pinho Brasil Junior
University of Brasilia. Mechanical Engineering Department. Energy and Environmental Laboratoty. 70910-900 Brasilia. DF. Brazil
antonio.no95@gmail.com, nelamacmac@gmail.com, taygoara@unb.br, brasiljr@unb.br

Abstract. This work presents an investigation of fish swimming using computational fluid dynamics with a quasi-steady flow approach. A tridimensional tuna motion model is analyzed for different time steps in an full swim cycle with this approach. Several geometries of the tuna fish were created based on a motion model, one for each time step. The parameters for each simulation were a steady flow condition and the k-ω turbulence model, using the ANSYS^{TM} Fluent solver. The final results were components of the drag force (components of pressure field and friction) and for a full period oscillation of the fish's tail and body and a time regression was made. These results were then compared to the values of the same conditions simulation and model found in previous paper regarding the same matter, but with a transient simulation approach.

Keywords: cfd, biomechanics, fish swimming, ansys fluent;

1. INTRODUCTION

Hydrokinetic turbines are machines capable of converting the kinetic energy in rivers flows into electric energy. This kind of energy transformation has been used since water wheels (Brasil Junior et al.,2007). However, transforming kinetic energy to electricity is still a somewhat new technology that has unknown, and yet to be studied and quantified, impacts.

In literature are described the main reasons which affect to aquatic life due to the installation of hydrokinetic devices highlighting sediment suspension, alteration of river hydraulic regimes, noise, electromagnetic fields and collisions of fish with blades, chemical toxicity and impacts due to installation and operation (Jordan et al., 2018; Musa et al., 2018; Daneshvar et al., 2017; Schramm et al., 2017; Zhang et al., 2017, Bonar and Bryden, 2015).

Most of works in this area study the collisions between fish and turbines. Experimental and numerical works are found in literature evaluating survival and damage rates (Wilson et al., 2007; Amaral et al., 2015; Castro-Santos and Haro, 2013; Romero-Gomez and Richmond, 2014; Zangiabadi et al., 2017).

To further understand this issue, comprehend the biomechanics and hydrodynamics of swimming organisms is necessary to analyze its interaction with the turbine and the wake flow induced by it. In literature, the hydrodynamic interaction between fish and turbine is explored poorly. In this work a study of a fish swimming in a undisturbed flow, without the turbine effect, is carried out to understand tits kinematic and hydrodynamic.

Studies based on fish swimming in undisturbed flow are common in the literature since 1960s. Experiments using the PIV techniques are realized to characterized fish swimming in undisturbed flows (Lighthill, 1971; Müller et al., 2001; Kern and Koumoutsakos, 2016). More recently, numerical studies have been conducted using different methodologies like painels method (Barrett et al., 1999; Najafi and Abbaspour, 2016), immersed boundary methods (Borazjani and Sotiropoulos, 2008; Borazjani and Sotiropoulos, 2009; Cui et al., 2017) or SPH method, *smoothed-particle hydrodynamics*, (Munnier and Pinçon, 2010). In these studies, the flow is in laminar regime or is considered as a potential flow. Liu et al. (2017) there are few works employing simulations with fish swimming in viscous flow with high Reynolds number where is necessary to resolve the problem of turbulence. Few works using the Unsteady Average Navier-Stokes (URANS) to model turbulence are found and the more common turbulence model used are the k-ω turbulence model (Adkins and Yan, 2006), k-ε turbulence model (Chang et al., 2012) and k-ω -SST turbulence model (Li et al., 2017).

This work presents a hydrodynamics analysis of the tuna motion, with a different approach regarding the Computer Fluid Dynamics (CFD) simulation. Instead of a transient analysis, several frames of the motion will be simulated using a permanent flow condition, for a full oscillation period (*quasi*-steady approach). The tuna and its motion parameters

are based in the work of Zhu et al. (2002). A comparison of the results obtained with the quasi-steady approach and the transient approach then is made to verify the accuracy of this simplified method of simulation.

2. TUNA MOTION KINEMATICS AND GEOMETRY

Swim motion involves the transference of momentum from the body to the fluid surrounding the body moving. This motion generates the resulting force that propels the body (Sfakiotakis et al., 1999). This motion can be both periodic oscillation, associated with big distances locomotion and unsteady rapid movements, associated with scape and hunting movements.

The tuna fish is part of a fish classification in which a wave with variable amplitude propagates along the body, from the head all the way to the fin. The wave amplitude is much greater near the tail region and the head region practically stays motionless. Most of the movement stays within the tail and caudal region. Such type of fish is categorized as thunninform.

The Reynolds number (Re) must be taken in consideration, for this kind of fish locomotion, as it is associated with turbulent flows and inertial regimes. Values between 10^4 and 10^6 are most common for this kind of fish. Due to the periodic motion, the Strouhal number (St) is a significant variable as well. For thunninforms, there is an optimal performance for values of St varying from 0,2 up to 0,4, for the Re range described above (Borazjani and Sotiropoulos, 2008). Both dimensionless groups, Re and St are calculated by the Eq. 1 and Eq. 2, respectively.

$$Re = \frac{\rho U L}{\mu} \tag{1}$$
$$St = \frac{f A}{U} \tag{2}$$

For Eq. 1, ρ is the density of the fluid in the flow, U is the fluid velocity, L is the characteristic length of the flow and μ is the viscosity of the fluid. For Eq. 2, f is the frequency of the oscillation; A is the maximum amplitude of the movement and U the velocity of the flow.

The tuna geometry was based in the work of Zhu et al. 2002 and presented in the Eq. 3 and Eq. 4 for the body and Eq. 5 and Eq. 6 for the caudal fin. In the equation, z is de height coordinate, x is the dorsal coordinate and L is the length from the head to the caudal peduncle, adopted as unitary.

$$z(x)/L = \pm 0,152 \tanh(6x/L + 1,8) \quad for \ -0,3 \le x/L \le 0,1 \tag{3}$$

$$z(x)/L = \pm(0,075 - 0,076 \tanh(7x/L + 3,15)) \quad for \ 0,1 < x/L \le 0,7 \tag{4}$$

$$x(z)_{LE}/L = 39,543|z/L|^3 - 3,685(z/L)^2 + 0,636|z/L| + 0,7 \quad for -0,15 \le z \le 0,15 \tag{5}$$

$$x(z)_{BF}/L = 40,74|z/L|^3 - 9,666(z/L)^2 + 0,77 \quad for -0,15 \le z \le 0,15 \tag{6}$$

Figure1 illustrates the lateral profile of the tuna fish as described in the previous equation. The blue part represents Eq. 3 and Eq. 4 and the red part, Eq. 5 and Eq. 6. The three dimensional modal is made by ellipses with aspect ratio of 1.5 alongside de body and a NACA 0016 on the tail region. Figure 2 illustrates the geometry of the tuna without any movement considered yet.
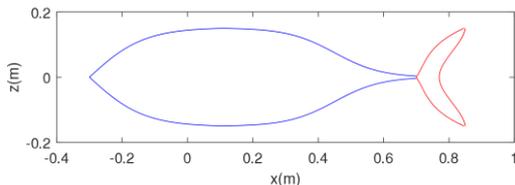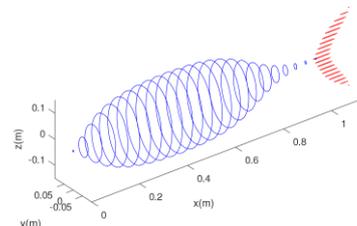

Figure 1. Tuna fish lateral profile

Figure 2. Tuna three dimensional curves

With the geometry well described by curves, the kinematics of the tuna fish, as shown in the work of Zhu et al., 2002 follows. A sinusoidal wave propagated alongside the tuna is described by the Eq. 7 and Eq. 8, and the caudal fin angle is determined by the Eq. 9.

$$y(x,t) = a(x)\sin(k_w x - \omega t) \tag{7}$$

$$a(x) = c_1 x + c_2 x^2 \tag{8}$$

$$\theta(t) = \alpha \sin(k_w x_p - \omega t - \varphi) \tag{9}$$

In Eq. 7, y is the amplitude, x the coordinate of the tuna's dorsal, t is time, k_w is the wave number, defined as $2\pi/\lambda$ (λ being the wave length), ω is the angular frequency. In Eq. 8, c_1 and c_2 are parameters that adjust the motion. Finally, in Eq. 9, θ is the angle of the fin and the x axis, α is the maximum angle of attack of the fin, x_p is the coordinate of the caudal peduncle and φ is the tail phase.

For this work, all these parameters were set accordingly to the 5th case of Zhu's work in order to obtain a St close to 0.3 and a Re of 7×10^5, as mentioned to be the ideal condition for generating thrust with oscillating motion.

In the Tab. 1 are presented all parameters used in the simulations.

Table 1. Parameters defining the fish kinematics

Strouhal number St	0.281
Swim speed (m/s)	0.7
Wave lenght λ (m)	1.297
Oscillation frequency ω (rad/s)	8.390
Maximun attack angle α (°)	17.77
Tail phase φ (°)	97.7
Amplitude coefficient c_1	0.00042
Amplitude coefficient c_2 (m^{-1})	-0.108
Maximum tail displacement A (m)	0.147
Oscillation period T (s)	0.7489

With the kinematics well established, the period of time for a complete oscillation is approximately 0,75 seconds. This interval was divides equally in twenty parts and twenty geometries were created in SOLIDWORKS^{TM}. The Fig. 3 presents the first time step geometry and the Fig. 4 show all geometries used to represents a cycle of the fish movements.

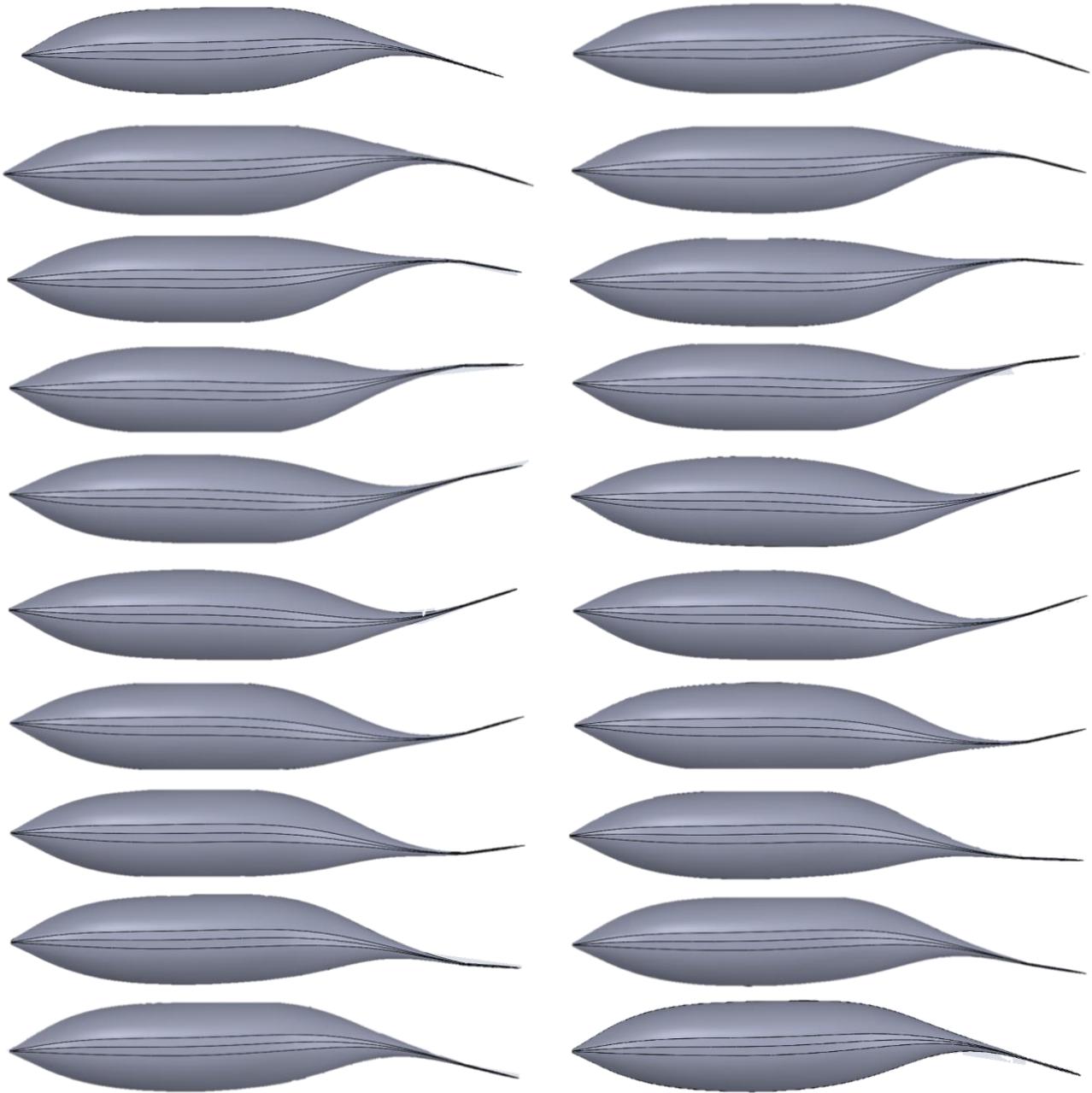Figure 3. Three dimensional model of the first time step

Figure 4. Twenty fish geometries in frontal view.

3. NUMERICAL METHOD AND SIMULATION SETUP

As mentioned, the ANSYS^{TM} Fluent solver was used to simulated the twenty different geometries. The software solves numerically the equations of continuity and momentum of fluid dynamics. In this work, the turbulence k-ω standard model (Wilcox, 1998) was applied. Equation 10 describes the mass conservation, Eq. 11 the momentum conservation. In Eq. 10 and Eq. 11, ρ is fluid density, t is time, x is the coordinates in indicial notation, p is pressure, μ is viscosity and δ is the Kronecker delta.

$$\frac{\partial \rho}{\partial t} + \frac{\partial (\rho u_i)}{\partial x_i} = 0 \tag{10}$$

$$\frac{\partial (\rho u_i)}{\partial t} + \frac{\partial (\rho u_i u_j)}{\partial x_j} = -\frac{\partial p}{\partial x_i} + \frac{\partial}{\partial x_j}\left[\mu\left(\frac{\partial u_i}{\partial x_j} + \frac{\partial u_j}{\partial x_i} - \frac{2}{3}\delta_{ij}\frac{\partial u_j}{\partial u_j}\right)\right] + \frac{\partial}{\partial x_j}\left(-\rho \overline{u'_i u'_j}\right) \tag{11}$$

A prismatic fluid domain was created with 7 meters in the direction of the flow, and a section of 2,5 by 2,5 meters transverse. Two influence cylinders were created for mesh refinement purposes. The final result of the geometry is show in Fig. 5. The Fig. 6 shows the refined mesh, with different element sizes in both cylinders and inflation on the tuna surface.

A complete mesh convergence study was realized studying the influence of the domain size and the density of elements in the different regions of refinement monitoring the drag force on the fish. The final parameters employed during the simulations are present in the Tab. 2. In Tab. 3 are presented the number of elements and nodes utilized in each time analyzed during the cycle.

Tab. 2. Final values of the main parameters in the numerical mesh

Element size (major cylinder)	5e-02 m
Element size (minor cylinder)	1e-02 m
Inflation (aspect ratio)	10
Inflation (layer number)	15
Inflation (growth rate)	1,05

Tab. 3. Number of elements and nodes to each mesh generated

|	Time(s)	Nodes	Elements
1	0,000	973740	3527244
2	0,039	972493	3516505
3	0,079	956878	3481267
4	0,118	960391	3488146
5	0,158	970632	3513751
6	0,197	962578	3489608
7	0,236	960630	3489569
8	0,276	968010	3512813
9	0,315	967866	3511813
10	0,355	965329	3500928
11	0,394	964248	3494772
12	0,434	965843	3500548
13	0,473	966579	3506983
14	0,512	971696	3523981
15	0,552	966179	3506008
16	0,591	965678	3504264
17	0,631	968370	3509276
18	0,670	964214	3497532
19	0,709	969640	3512589
20	0,749	971881	3514776
Average		966643,75	3505118,65
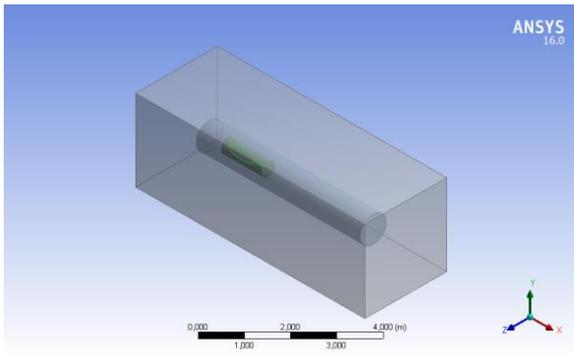
Figure 5. Final Ansys Simulation Geometry
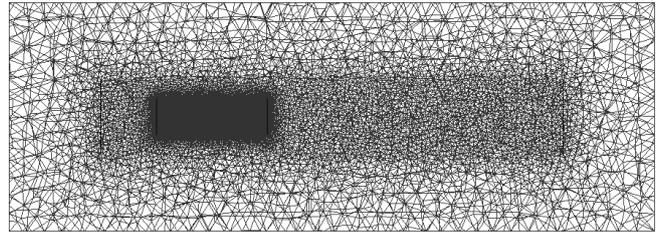
Figure6. Refined mesh used on all simulations

The setup and boundary conditions were inlet velocity of 0.7 m/s, no shear in the walls of the fluid domain, no slip condition on the surface of the tuna and atmospheric pressure on outlet.

4. RESULTS

After all the time steps were simulated, information of total drag was collected, which includes pressure field component and viscous shear component. A time regression and a time average of the result of pressure and viscous forces was also made.

The forces in x and z direction were analyzed and the force component in y was neglected because the geometries are symmetric in relation to the plane xz. In Tab. 5 and Tab. 6 are presented the hydrodynamics forces in form of pressure and viscous forces for the instants of time analyzing in directions x and z, respectively.

A regression curve to the forces function of the time was realized to obtain the force behavior during a oscillation period. The function has the form $F(t) = Asin(\omega t + \varphi) + B$.

Table 5. Force component in x direction.

Fx (N)			
Time (s)	Pressure	Viscous	Resultant
0,000	1,122	0,695	1,816
0,039	1,200	0,693	1,894
0,079	1,108	0,694	1,802
0,118	0,886	0,695	1,581
0,158	0,608	0,700	1,308
0,197	0,297	0,779	1,076
0,236	0,276	0,733	1,009
0,276	0,426	0,724	1,150
0,315	0,772	0,710	1,482
0,355	1,058	0,699	1,757
0,394	1,196	0,695	1,891
0,434	1,162	0,691	1,853
0,473	1,004	0,695	1,699
0,512	0,738	0,694	1,432
0,552	0,499	0,715	1,214
0,591	0,229	0,801	1,030
0,631	0,266	0,781	1,047
0,670	0,638	0,705	1,343
0,709	0,937	0,702	1,639
0,749	1,141	0,696	1,837

Table 6. Force component in z direction.

Time (s)	Pressure	Viscous	Resultant
	Fz (N)		
0,000	-2,226	0,010	-2,216
0,039	-2,188	0,011	-2,177
0,079	-1,990	0,012	-1,978
0,118	-1,678	0,010	-1,668
0,158	-1,283	0,008	-1,275
0,197	-0,731	0,003	-0,729
0,236	0,353	0,002	0,355
0,276	1,535	-0,001	1,533
0,315	2,187	-0,005	2,182
0,355	2,315	-0,008	2,306
0,394	2,299	-0,011	2,288
0,434	2,048	-0,012	2,037
0,473	1,823	-0,012	1,811
0,512	1,416	-0,010	1,406
0,552	1,388	-0,006	1,383
0,591	-0,907	0,002	-0,904
0,631	-1,137	0,001	-1,136
0,670	-1,898	0,002	-1,896
0,709	-2,300	0,007	-2,293
0,749	-2,281	0,010	-2,271

Main parameters in both regression curves, in x and z, are frequency and amplitude. In direction x, the amplitude obtained was 0.44N and frequency 16.89 rad/s. This value is approximately twice the frequency of tuna movement equal to 8.39 rad/s. This result was expected due to the tuna movement is symmetric in relation to x axis. The equation for the drag force in Newtons in a full oscillation is described in Eq. 12 and represented in Fig. 7.
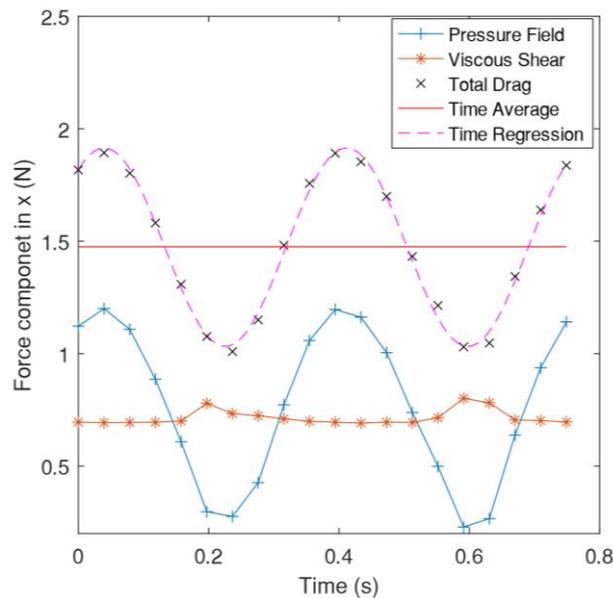
$$F_x(t) = 0.44sin(16.89t + 0.90) + 1.47 \tag{12}$$

Figure 7. Forces in x direction

On the other hand, in direction z, it was computed an amplitude equal to 2.29 N and a frequency of 8.96 rad/s. Therefore, the value obtained is very close to the swimming oscillation frequency value. In this case, the force in z presented only one peak due to the movement is not symmetric in relation to axis z. The Eq. 13 show the parameters defining the regression curve to the drag force in z direction and the Fig. 9 present the curves obtained.

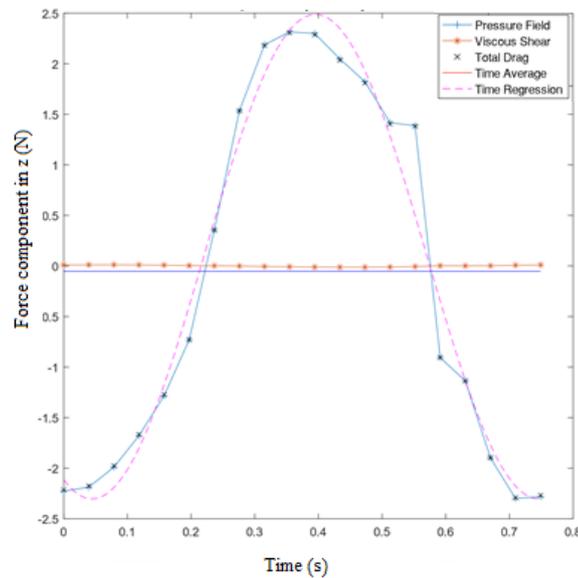$$F_z(t) = 2.39sin(8.96t - 1,97) + 0.09 \tag{13}$$

Figure 9. Forces in z direction

Finally, the resulting force, F_T, computed as the vector sum is presented, graphically in Fig. 9 and in form of equation in Eq. 14.

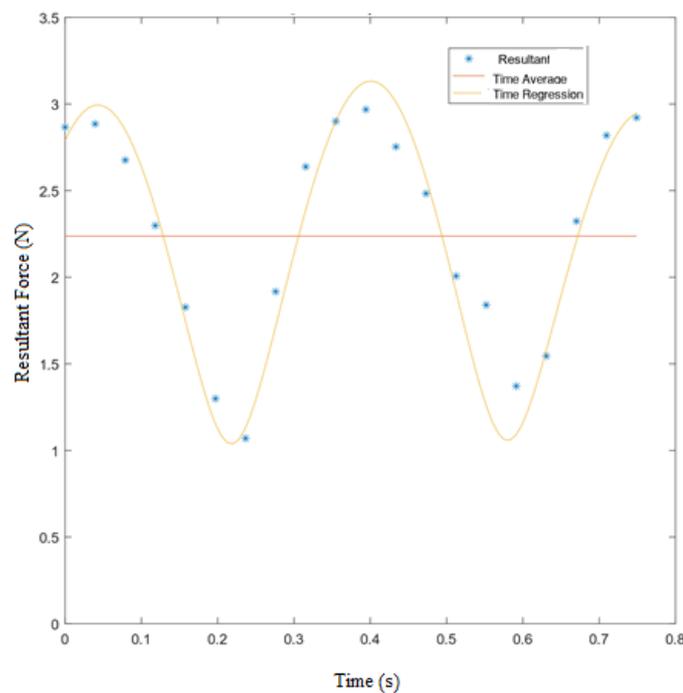$$F_T(t) = 0.969sin(17.34t + 0.907) + 2.162 \tag{14}$$

Figure 10. Resulting forces.

The average drag force, in x, in a full oscillation is 1.48 N. Zhu et al. (2002) obtained a value of 2.24 N numerically using a transient formulation and the same parameters. There is a 34% relative difference between the two approaches, which is rather small taking in consideration how simplified the quasi-steady method is compared to the transient formulation. See Fig. 7.

In direction z, the temporal average obtained was -0.053N which can be considered zero if compared to the others values obtained, Fig. 8. The forces in direction z change the magnitude and sense according to the caudal fin movement, symmetric during a complete oscillation period. An expected result in the analyze.

The total power for the thrust obtained was 1.56 W. Again, comparing with the work of Zhu et al. (2002), which obtained 2.45 W, there is a relative error of 36%, very close to the error obtained for the force in the x direction.

In the simulations, the swim speed is considered constant in the time and therefore, there must be a static balance of forces. The propulsive force, in forward flow direction, has to be equal that the drag force, in the direction of the flow. It is important to note that in the quasi-static analyze the force computed is the drag force and not the propulsive force.

5. CONCLUSION

With the results obtained, it can be concluded that although the quasi-steady and the transient methods have different results, the relative distance between the values obtained are acceptable when taken in consideration the great simplification of the method used in this work. Thus, in terms of simplification and estimates, the quasi-steady approach has results that can be used.

For more accurate results, more time steps can be used other than the twenty chosen for this work. After the algorithm for the geometry curves is set, the parameters can be easily changed and other cases of the work of Zhu et al. (2002) can also be tested and compared.

Finally, it is important to conclude that using this method the force obtained with the numerical simulations in the flow direction is the drag force. Therefore, the propulsive force only could be considered equal to the drag in the case of static balance when the speed swim is constant.

6. REFERENCES

Adkins, D.; Yan, Y. Y. CFD Simulation of Fish-like Body Moving in Viscous Liquid. Journal of Bionic Engineering, 2006. ISSN 16726529.

Amaral, S. V. et al. Evaluation of Behavior and Survival of Fish Exposed to an Axial-Flow Hydrokinetic Turbine. North American Journal of Fisheries Management, v. 35, n. 1, p. 97–113, 2015. ISSN 0275-5947.

Bonar, Paul AJ, Ian G. Bryden, and Alistair GL Borthwick. "Social and ecological impacts of marine energy development." Renewable and Sustainable Energy Reviews47 (2015): 486-495.

Barrett, D. S. et al. Drag reduction in fish-like locomotion. Journal of Fluid Mechanics, v. 392, p. 183–212, 1999. ISSN 1469-7645.

Borazjani, Iman, and Fotis Sotiropoulos. "Numerical investigation of the hydrodynamics of carangiform swimming in the transitional and inertial flow regimes." Journal of Experimental Biology 211.10 (2008): 1541-1558.

Castro-Santos, T.; Haro, A. Survival and Behavioral Effects of Exposure to a Hydrokinetic Turbine on Juvenile Atlantic Salmon and Adult American Shad. Estuaries and Coasts, 2013.

Chang, X.; Zhang, L.; He, X. Numerical study of the thunniform mode of fish swimming with different Reynolds number and caudal fin shape. Computers and Fluids, Elsevier Ltd, v. 68, p. 54–70, 2012. ISSN 00457930.

Cui, Z. et al. CFD Studies of the Effects of Waveform on Swimming Performance of Carangiform Fish. Applied Sciences, v. 7, n. 2, p. 149, 2017.

Daneshvar, F. et al. Applications of computational fluid dynamics in fish and habitat studies. Ecohydrology and Hydrobiology, European Regional Centre for Ecohydrology of the Polish Academy of Sciences, v. 17, n. 1, p. 53–62, 2017.

Jordan, L. B. et al. Laboratory study on the effects of hydro kinetic turbines on hydrodynamics and sediment dynamics. Renewable Energy, Elsevier Ltd, v. 129, p. 271–284, 2018.

Junior, A.C.P.B, et al. "Turbina Hidrocinética Geração 3." IV CONGRESSO. 2015.

Kern, S.; Koumoutsakos, P. Simulations of optimized anguilliform swimming. Journal of Experimental Biology, v. 209, n. 24, p. 4841–4857, 2006. ISSN 0022-0949.

Lighthill, J. . Large-Amplitude Elongated-Body Theory of Fish Locomotion. Royal Society, v. 179, n. 1055, p. 125–138, 1971.

Liu, G. et al. Computational analysis of vortex dynamics and performance enhancement due to body-fin and fin-fin interactions in fish-like locomotion. Journal of Fluid Mechanics, v. 829, p. 65–88, 2017. ISSN 14697645.

Müller, U. K. et al. How the body contributes to the wake in undulatory fish swimming: flow fields of a swimming eel (Anguilla anguilla). The Journal of experimental biology, v. 204, n. Pt 16, p. 2751–62, 2001. ISSN 0022-0949.

Munnier, A.; Pinçon, B. Locomotion of Articulated Bodies in an Ideal Fluid: 2D Model With Buoyancy, Circulation and Collisions. Mathematical Models and Methods in Applied Sciences, v. 20, n. 10, p. 1899–1940, 2010.

Musa, M. et al. Performance and resilience of hydrokinetic turbine arrays under large migrating fluvial bedforms. Nature Energy, Springer US, v. 3, n. 10, p. 839–846, 2018. ISSN 20587546.

Najafi, S.; Abbaspour, M. Numerical Study of Propulsion Performance in Swimming Fish using Boundary Element Method. Journal of the Brazilian Society of Mechanical Sciences and Engineering, 2016.

Romero-Gomez, P.; Richmond, M. C. Simulating blade-strike on fish passing through marine hydrokinetic turbines. Renewable Energy, n. 71, p. 401–4013, 2014.

Schramm, M. P.; Belvelhimer, M.; Scherelis, C. Effects of hydrokinetic turbine sound on the behavior of four species of fish within an experimental mesocosm. Fisheries Research, v. 190, p. 1–14, 2017. ISSN 01657836.

Sfakiotakis, Michael, David M. Lane, and J. Bruce C. Davies. "Review of fish swimming modes for aquatic locomotion." IEEE Journal of oceanic engineering 24.2 (1999): 237-252.

Wilcox, David C. *Turbulence modeling for CFD*. Vol. 2. La Canada, CA: DCW industries, 1998.

Wilson, B. et al. Collision risks between marine renewable energy devices and mammals, fish and diving birds. Oban, Oban, n. March, p. 110, 2007.

Zangiabadi, E. et al. Computational prediction of pressure change in the vicinity of tidal stream turbines and the consequences for fi sh survival rate. Renewable Energy, v. 101, p. 1141–1156, 2017. ISSN 09601481.

Zhang, J. et al. Impact assessment of marine current turbines on fish behavior using an experimental approach based on the similarity law. Journal of Marine Science and Technology (Japan), Springer Japan, v. 22, n. 2, p. 219–230, 2017. ISSN 09484280.

Zhu, Q., et al. "Three-dimensional flow structures and vorticity control in fish-like swimming." Journal of Fluid Mechanics 468 (2002): 1-28.

7. RESPONSIBILITY NOTICE

The author(s) is (are) the only responsible for the printed material included in this paper.